

Estimation of the spatial distribution of traps using space-charge-limited current measurements in an organic single crystal

Javier Dacuña

Department of Electrical Engineering, Stanford University, Stanford, California 94305, USA

Wei Xie

Department of Chemical Engineering and Materials Science, University of Minnesota, Minneapolis, Minnesota 55455, USA

Alberto Salleo*

Department of Materials Science and Engineering, Stanford University, Stanford, California 94305, USA

(Received 8 July 2012; published 6 September 2012)

We used a mobility edge transport model and solved the drift-diffusion equation to characterize the space-charge-limited current of a rubrene single-crystal hole-only diode. The current-voltage characteristics suggest that current is injection-limited at high voltage when holes are injected from the bottom contact (reverse bias). In contrast, the low-voltage regime shows that the current is higher when holes are injected from the bottom contact as compared to hole injection from the top contact (forward bias), which does not exhibit injection-limited current in the measured voltage range. This behavior is attributed to an asymmetric distribution of trap states in the semiconductor, specifically, a distribution of traps located near the top contact. Accounting for a localized trap distribution near the contact allows us to reproduce the temperature-dependent current-voltage characteristics in forward and reverse bias simultaneously, i.e., with a single set of model parameters. We estimated that the local trap distribution contains $1.19 \times 10^{11} \text{ cm}^{-2}$ states and decays as $\exp(-x/32.3 \text{ nm})$ away from the semiconductor-contact interface. The local trap distribution near one contact mainly affects injection from the same contact, hence breaking the symmetry in the charge transport. The model also provides information of the band mobility, energy barrier at the contacts, and bulk trap distribution with their corresponding confidence intervals.

DOI: [10.1103/PhysRevB.86.115202](https://doi.org/10.1103/PhysRevB.86.115202)

PACS number(s): 72.80.Le, 71.20.Rv

I. INTRODUCTION

Charge transport in organic single crystals has been the subject of numerous studies during the last decades.¹⁻⁵ Single crystals, with their high chemical purity and low defect density, stand as the perfect candidates to analyze and understand the fundamental limitations of charge transport in organic semiconductors. This understanding is an important requirement in order to move forward in the rationalization of the design of improved materials. Furthermore, measurements done on well-defined single crystals allow us to test transport and measurement models that can then be confidently extended to more complicated materials.

The analysis of the space-charge-limited current (SCLC) in hole- or electron-only organic devices is a common technique used to obtain information regarding the mobility and trap distribution in the transport gap.^{2,3,6-10} The utilization of accurate models that include all the physical effects that influence the charge transport in a SCLC measurement is very important in order to obtain accurate information about all the materials and interfaces involved. Parameters such as the energy barrier at the metal-semiconductor interface or the diffusion current, both of which are usually neglected in simple analytical models, have been shown to be important in the analysis of SCLC data.^{11,12}

The simplest configuration for SCLC measurements is the “sandwich” configuration, in which a voltage is applied to contacts on opposite sides of an organic single-crystal slab. In this case, provided that the length in the transport direction is

small compared to the other two dimensions, the device can be treated as a one-dimensional system and simple analytical or numerical methods can be used in the analysis.

During the preparation of the device for SCLC measurements, contacts are fabricated in such a way that at least one of them efficiently injects one type of carrier,¹³ while the other blocks the opposite polarity carrier. Injection of carriers from the low-energy barrier contact is then measured as a function of the applied voltage and temperature. Conversely, injection from the high-energy barrier contact is usually not analyzed since the injection mechanism from the contact to the semiconductor limits the current, thus reducing the voltage and temperature range where the current is limited by the transport properties of the organic material. This limitation increases the complexity of the analysis, in particular if analytical models are to be used.

Alternatively, numerical models that include the contact details should be able to reproduce both bias polarities; hence the reverse bias current can be used to improve the estimation of the parameters being analyzed. Furthermore, the analysis of the reverse bias current provides a way of validating some of the assumptions on which the model relies. In particular, a common assumption in SCLC models is the semiconductor homogeneity in terms of trap distribution. The nonhomogeneity of the trap distribution has been shown in the past to cause asymmetries in the current-voltage (I-V) characteristics as a function of the applied polarity.^{14,15}

In this work we show that the homogeneity assumption does not agree with experimental measurements of a rubrene single

crystal in which gold has been used as the bottom contact and silver has been used as the top contact. Modeling the complete I-V characteristics, i.e., including injection from both top and bottom contacts, requires taking into consideration a localized distribution of traps near one of the two electrodes. The proposed model improves the estimation of the bulk trap distribution, band mobility, and contact energy barriers. Additionally, it provides an estimation of the local trap density near the contacts as well as its spatial distribution. This last finding is very important in order to understand the physical origin of trap states in the transport gap.

II. EXPERIMENTAL

A. Device fabrication

Single crystals of rubrene were grown by horizontal physical vapor transport.¹⁶ Ultrapure argon was used as the carrier gas. Typical growth temperature was 300 °C. Platelike crystals a few millimeters wide and long and a few hundred nanometers thick were collected after a ~30 min growth and were immediately laminated on a clean Si wafer with prefabricated Cr (3 nm)/Au (30 nm) electrodes. Bottom contact was thus formed through spontaneous adhesion of thin crystals on an Au electrode.

Conversely, the top contact was prepared by depositing Leitsilber 200 silver paint (Ted Pella) on the top surface of the crystal. Charge transport occurs in the out-of-plane direction, i.e., along the longest axis of the orthorhombic unit cell.^{4,17,18}

B. Electrical characterization

Current was measured at different temperatures in vacuum (10^{-4} mbar) and in the dark, using a Keithley 6487 picoammeter. The device was cooled to 250 K and measurements were taken by increasing the temperature in 10 K steps. The complete measurement procedure was repeated twice to ensure that the device did not show any electrical stress and I-V measurements were reproducible. The I-V curves show asymmetric behavior, depending on the polarity of the applied voltage, caused by the differences between the top and bottom contact-semiconductor interfaces.¹⁹

Injection of holes from the bottom (laminated) contact exhibits injection-limited current for voltages higher than ~4 V, while the top (silver ink painted) contact does not suffer from injection problems. We refer to injection of holes from the bottom contact as reverse bias, and injection from the top contact as forward bias.

We note however that the current in the forward biased condition at low voltage, however, is lower than in the reverse biased condition by more than one order of magnitude at certain voltages and temperatures. Figure 1 compares the forward and reverse bias currents for the lower and higher temperatures measured (the complete set of temperature-dependent measurements is presented in Fig. 6). This behavior does not agree with the simple picture of a perfectly homogeneous semiconductor sandwiched in between two contacts with slightly different energetic barriers. Indeed, in a homogeneous semiconductor at a given temperature and voltage, the current measured when injecting carriers from the

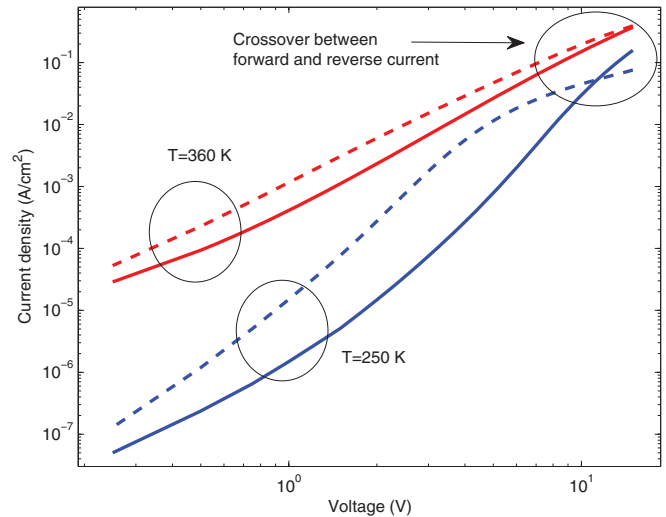


FIG. 1. (Color online) Comparison of forward (solid line) and reverse (dashed line) bias conditions at the maximum and minimum temperatures measured in this study, and detail of the crossover of the two curves.

higher-barrier contact should be smaller than that measured when injection occurs from the lower-barrier contact.

It is worth noting at this point that the forward I-V curves alone are perfectly reasonable and can be reproduced by using a homogeneous semiconductor in the numerical model. However, as explained later, this would introduce an error in the estimated parameters and, of course, the information on the spatial distribution of traps would be lost.

III. MODELING AND PARAMETER EXTRACTION

A. Model description

The I-V characteristics at different temperatures through the semiconductor were calculated using a numerical drift-diffusion model.¹¹ While the details of the numerical model are explained in Ref. 11, a brief description of the parameters and important aspects of the model is included here for completeness.

Charge transport is described using the mobility edge (ME) model,²⁰ which is believed to correctly describe charge transport in polycrystalline and single-crystal materials.^{21–25} The ME model divides the density of states (DOS) into mobile and localized states which are below and above the ME, respectively, in a hole transport semiconductor. Charges in mobile states drift under the influence of an electric field with mobility μ_0 , while charges in localized states are, by definition, nonmobile.

The numerical model accounts for the energetic barrier at the contact-semiconductor interface by fixing the difference between the ME and the Fermi-level position at the contacts (ϕ_t and ϕ_b for the top and bottom contact, respectively).

The energy distribution of the trap states in the bulk of the semiconductor is defined as a piecewise exponential; i.e., it varies exponentially in between every two neighboring energy points chosen for the trap distribution discretization. The values of the trap density at these points are parameters of the model. The density of mobile states in the band (below ME)

is assumed to be constant^{11,26} and equal to $10^{21} \text{ cm}^{-3} \text{ eV}^{-1}$. In addition, we define a localized trap distribution near the contacts as

$$\rho_{\text{trnc}}(E, x) = \frac{\alpha \exp(-x/\beta)}{\sqrt{2\pi\sigma^2}} \exp\left(-\frac{(E - E_c)^2}{2\sigma^2}\right). \quad (1)$$

The local trap distribution has Gaussian shape centered at E_c with standard deviation σ . It decays as $\exp(-x/\beta)$ away from the contact-semiconductor interface, and the total amount of trap states integrated from $x = 0$ to ∞ is $\gamma = \beta\alpha$. Although the exact spatial distribution is difficult to obtain from simple SCLC measurements, the utilization of a simple exponential captures the essential physics of the problem and allows us to obtain an estimation of the total concentration of traps and spatial extent.

Fits to the experimental measurements, and calculation of the confidence intervals, show that there is a strong correlation between E_c , σ , and γ , which results in very large confidence intervals for these parameters, that is, large uncertainties. The reason is that the model is not sensitive to the energetic distribution of this local trap density, which makes it difficult to obtain a reliable estimate of the actual shape or energetic position of the local traps. Consequently, E_c has been fixed to a value deep enough such that all the states in the localized trap distribution are occupied. As a consequence the actual parameters that characterize the local trap density in the model are γ and β , that represent the total density of active local traps near the contact and its spatial distribution, respectively. Therefore, the modeling of the electrical characteristics measured here does not provide any information of the energetic distribution of local traps near the contact, but only the spatial distribution of the density of active (i.e., occupied by holes) local trap states.

B. Effect of local traps near the contacts

Trap states in organic crystals can appear, among other effects, due to structural defects, chemical impurities, or defects generated by chemical reaction of the semiconductor with oxygen.²⁷ Although the concentration of trap states can be nonuniform through the semiconductor, most SCLC modeling efforts to date assume a homogeneous trap distribution. In a completely homogeneous and ideal hole-only device with perfect ohmic and symmetric contacts, the I-V characteristics have to be symmetric. In contrast, when a local trap density is present near one of the contacts, the charge density created by carriers trapped at these localized states will induce a strong band bending, breaking the symmetry of the device.

This strong band bending pushes the Fermi-level position away from the ME near the contact, thus reducing the effective density of free carriers in the device. Figure 2 compares the position of the ME and Fermi-level of an arbitrary device with no local traps, local traps at the injecting contact, and local traps at the extracting contact. Symmetric contacts and no bulk traps were considered in this example, thus the simulation without local traps follows the well-known $I \propto V^2$ behavior predicted by the Mott-Gurney equation (Fig. 4).

The presence of traps at the contacts has a strong impact on the overall density of free carriers through the entire

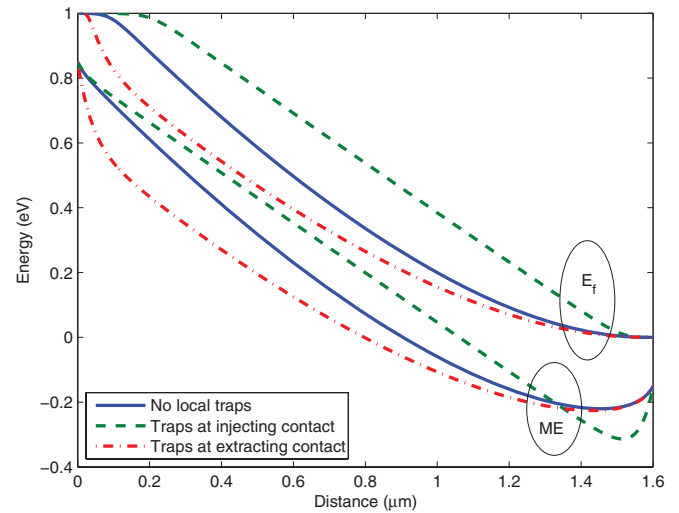


FIG. 2. (Color online) Mobility edge and Fermi-level position as a function of distance from the contacts for an applied voltage of 1 V. Holes are injected from the contact located at the right-hand boundary. Strong band bending is created near the contacts due to local traps, increasing the distance between the ME and Fermi level when traps are close to the injecting contact.

device, as shown in Fig. 3. The reduction of the density of free carriers implies a reduction on the current density (Fig. 4), which is dramatically different when carriers are injected from one contact or the other. The effect is particularly important at low voltage. At high voltage the density of injected carriers increases while that of the trapped carriers at the local trap distribution remains constant; hence the I-V behavior approaches the ideal case.

The effect of local traps also is temperature dependent, as shown in the inset of Fig. 4, and becomes more noticeable at low temperatures. The temperature dependence is very similar to the temperature dependence of the I-V curves for a bulk

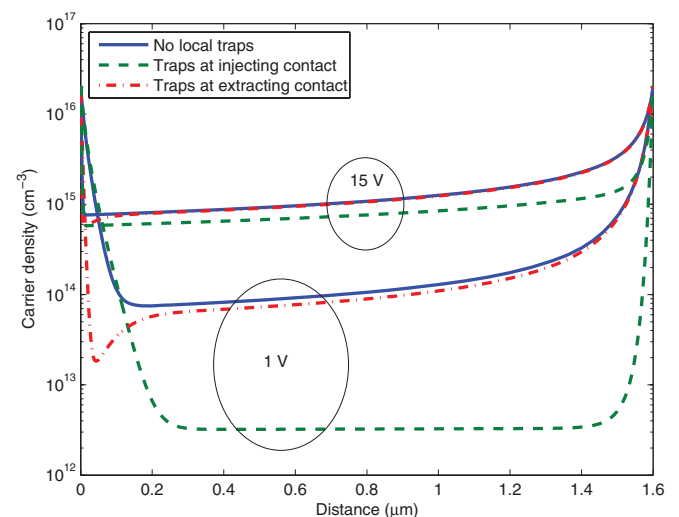


FIG. 3. (Color online) Free-carrier density distribution as a function of position. Holes are injected from the right. The density of free carriers is strongly reduced when local traps are present near the injecting contact. The effect is considerably smaller when traps are located at the opposite (extracting) contact.

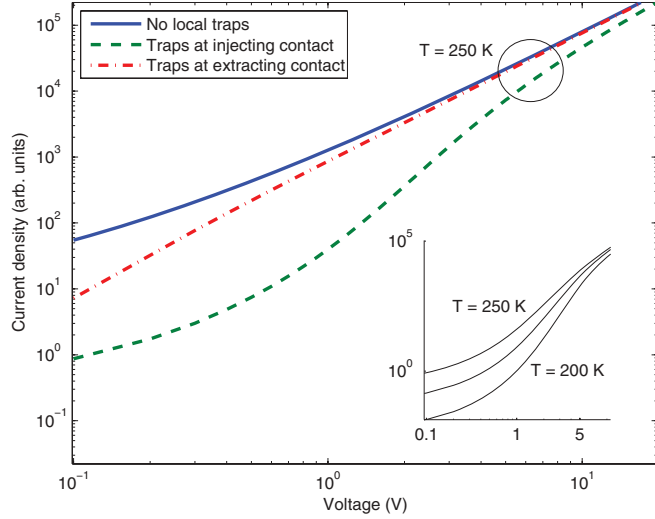


FIG. 4. (Color online) Effect of local traps on the I-V curve at 250 K. Inset: temperature dependence of the I-V characteristic when traps are close to the injecting contact.

traps-limited device. Hence experimental I-V curves for a single polarity (either forward or reverse bias, but not both simultaneously) can be reproduced with a model that does not account for local traps but only a homogeneous bulk trap distribution, at least in a limited voltage and temperature range, thus providing erroneous results.

C. Obtained parameters and confidence intervals

The parameters of the model have been estimated using least-squares optimization and their 95% confidence intervals have been calculated using the profile-likelihood method.^{11,28} A band mobility $\mu_0 = (3.55 \pm 0.05) \times 10^{-2} \text{ cm}^2/\text{V s}$ was found, consistent with transport along the slow-transport direction of the rubrene unit cell. The energy barrier at the contact is slightly higher for the bottom contact (laminated) interface, $\phi_b = (250 \pm 1) \text{ meV}$, as compared to the top contact (silver paint), $\phi_t = (189 \pm 8) \text{ meV}$.

The density of traps near the top contact was found to be $\gamma = (1.19 \pm 0.1) \times 10^{11} \text{ cm}^{-2}$, and decays far away from the interface with $\beta = (32.34 \pm 2.1) \text{ nm}$. Including a local trap distribution near the bottom contact resulted in a substantially lower trap density with large confidence intervals (both in density γ_{bottom} and spatial distribution β_{bottom}) and a negligible improvement in the fit. Thus, although we cannot claim that the bottom surface does not contain local traps, they certainly do not dominate the transport properties of the device.

Figure 5 (top) shows the obtained bulk trap distribution in the semiconductor. The energetic distribution of states deeper than $\sim 550 \text{ meV}$ cannot be resolved because they are always occupied at any measured voltage and temperature,¹¹ thus only the total integrated number of deep traps was determined (inset). Similarly, the occupation probability of states shallower than $\sim 250 \text{ meV}$ is very small, which leads to a small sensitivity of the model to states in this region and hence to a large uncertainty. Consequently, only the trap distribution in the energy range from 250 to 550 meV above the ME was determined. Due to the limited energy range and resolution,

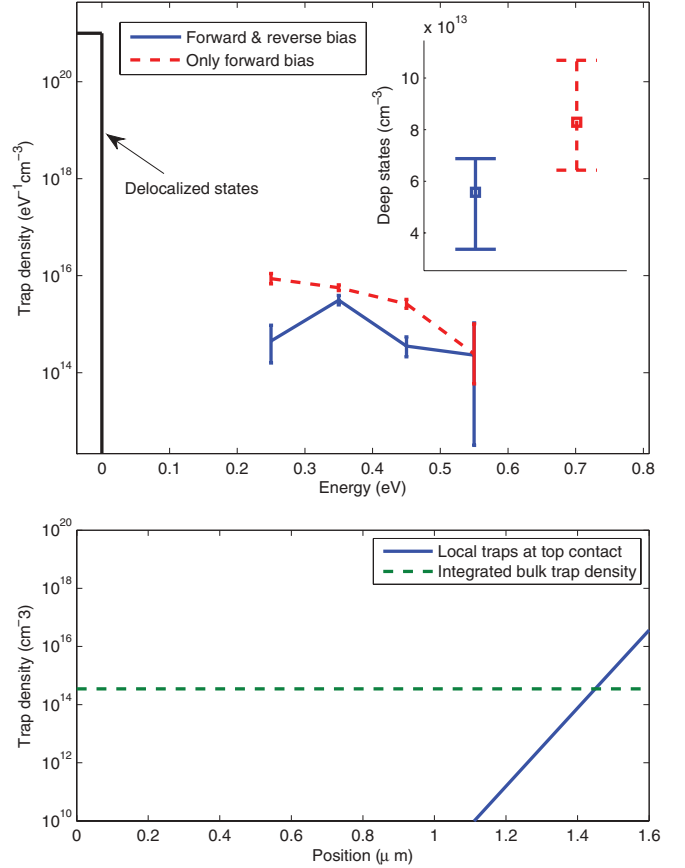


FIG. 5. (Color online) Top: energetic distribution of bulk traps obtained by least-squares fitting the forward and reverse I-V curves (solid lines) and only the forward bias I-V curves (dashed lines). Using only the forward bias, and neglecting localized traps at the contact, results in an overestimated bulk trap density. Vertical lines represent the 95% confidence intervals. Inset: integrated trap density for states deeper than 0.55 eV. Bottom: distribution of localized traps compared to the integrated bulk trap density.

it is not possible to determine the specific shape of the bulk density of trap states. Gaussian and exponential shapes are commonly used to characterize traps in organic materials.²⁹⁻³¹ The values we obtain are in reasonable agreement to DOS obtained previously for rubrene single crystals.^{10,11}

Figure 5 (bottom) compares the estimated density of local trap states, as a function of position, to the integrated density of bulk traps. The intersection between the two curves, approximately $\sim 150 \text{ nm}$ away from the interface, provides an estimation of the spatial extension of the local traps as compared to bulk traps.

Finally, Fig. 6 compares the experimental measurements to the model calculations. The model correctly reproduces the I-V characteristics for all temperatures and voltages, including the forward and reverse bias conditions.

D. Importance of local traps

As explained above, the set of forward bias I-V curves can be reproduced entirely using a homogeneous semiconductor in the numerical model. The obtained trap distribution in this case is shown in Fig. 5 with dashed lines. Since no localized traps

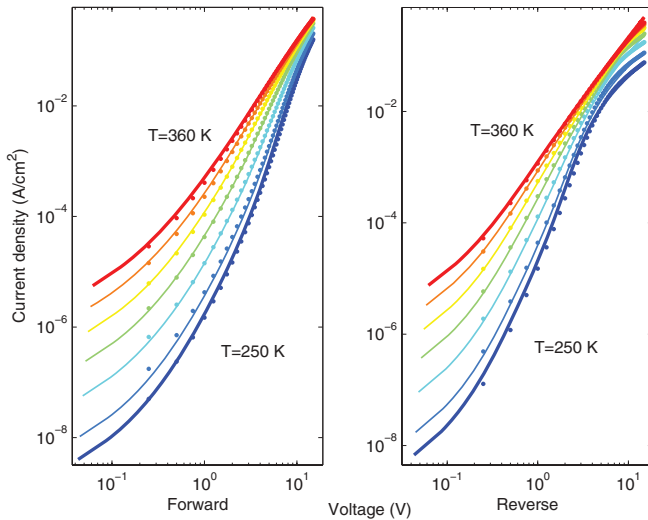


FIG. 6. (Color online) Comparison of the measured data (dots) and model (solid lines) for forward and reverse bias conditions at different temperatures.

are considered, the bulk trap distribution is overestimated in the entire energy range. Furthermore, the shape of the distribution is markedly different. Fitting only forward bias data produces a monotonically decreasing trap DOS while the complete model produces a slightly peaked DOS, which suggests the existence of a characteristic trap depth.

In addition to the error in the obtained trap distribution, fitting only the forward bias current also introduces a $\sim 20\%$ error in the estimated band mobility μ_0 , as shown in Table I. The estimation of the energetic barriers at the contacts is also affected. In particular, the estimated energy barrier at the bottom contact is reduced to 1/2 of the value and has large uncertainty.

Arguably the most important loss of information when neglecting the reverse bias I-V measurements in the data analysis is that the spatial information regarding local traps is not known. Indeed, if only the I-V characteristics corresponding to the forward bias condition are analyzed, it would be difficult to imagine that local traps are required since the assumption of a homogeneous semiconductor is sufficient to reproduce the measurements with reasonable parameters. The spatial information of the local traps is very important because it points to a completely different physical origin of these states, which limit the performance of our particular device, as compared to bulk traps.

Bulk traps can be caused by disorder, chemical or morphological defects, or impurities in the semiconductor material.²⁷ Therefore, they can be reduced by further purification or modification of the crystal growth conditions.³² In contrast,

TABLE I. Comparison of obtained parameters using forward and reverse bias currents (with bulk and local traps) and using only forward bias currents (with only bulk traps).

	μ (cm ² /Vs)	ϕ_t (meV)	ϕ_b (meV)
Complete	$(3.55 \pm 0.05) \times 10^{-2}$	(189 ± 8)	250 ± 1
Only forward	$(4.25 \pm 0.1) \times 10^{-2}$	(209 ± 8)	$110 (<157)$

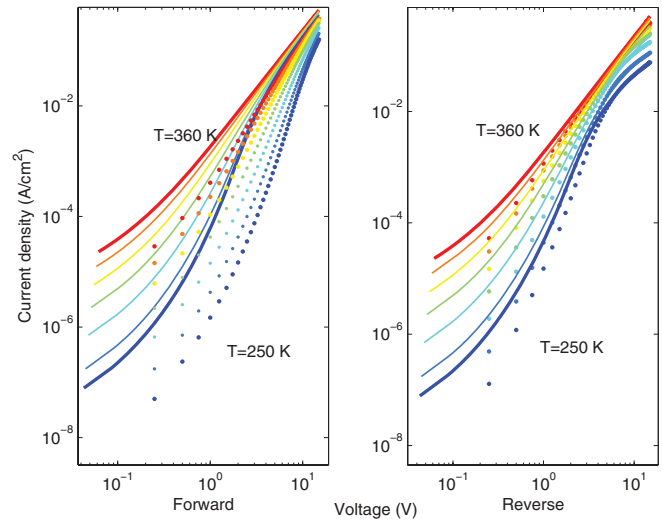


FIG. 7. (Color online) Comparison of I-V measurements and model calculations if the local traps are removed.

the local distribution of trap states found near the top contact is likely created by contaminants due to a longer exposure of the top surface of the crystal in an uncontrolled atmosphere, residual solvent molecules from the silver paint used to deposit the top contact, or oxygen-related traps that develop in molecular crystals after illumination in an oxygen atmosphere.^{33,34} In other words, bulk traps are related to the growth of the crystal while local traps are more linked to the manipulation of the crystal after growth and to the specific processing steps used in fabricating the contacts.

To further emphasize the importance of the local traps on the SCLC measurements, Fig. 7 compares the measured data to the model calculations if the local traps are removed. While the reverse bias condition remains relatively unaffected, the forward bias I-V curves are clearly limited by the presence of local traps.

IV. CONCLUSIONS

The study of charge transport in organic single crystals is important in order to understand the physical limitations that reduce the performance in organic semiconductor devices. Equally important, if not more important, is to determine the origin of these physical limitations in order to rationalize the design of semiconductors or fabrication methods that outperform the materials used today.

We have applied a numerical drift-diffusion model to characterize the SCLC measurements of a rubrene single crystal. The utilization of both forward and reverse bias conditions in the analysis of the SCLC measurements allows us to demonstrate that a common assumption made in several analytical and numerical models, namely, the homogeneity of the trap distribution in the semiconductor, is not valid. By incorporating a local trap distribution near the top (silver ink painted) contact, our model correctly reproduces the forward and reverse bias conditions over a range of different temperatures simultaneously, i.e., with a single set of model parameters.

The utilization of our complete model provides a more accurate estimation of common parameters such as the band mobility, the bulk trap density, and the energetic barriers at the contacts. In addition, it provides information regarding the amount and spatial distribution of localized traps. These local traps are thought to be caused by contamination of the top surface of the organic crystal or by photo-oxidation due to the longer exposure to an uncontrolled atmosphere after the crystal growth. Determining the origin of trap states, in addition to their concentration, is very important in order to rationalize the design of materials or processing techniques with improved electrical performance.

The model also provides the estimation of the confidence intervals of the parameters, which allows us to determine the variables that actually influence the I-V measurements and discard the ones that are not important. Namely, states

deeper than $\simeq 0.55$ eV cannot be energetically resolved and only their aggregate contribution was estimated. Likewise, the model is not sensitive to states shallower than ~ 0.25 eV and these are neglected. Traps located near the bottom (laminated) contact of the device do not significantly contribute to the I-V characteristics in this particular device.

ACKNOWLEDGMENTS

This paper was based on work supported by the Center for Advanced Molecular Photovoltaics (Award No. KUS-C1-015-21), made by King Abdullah University of Science and Technology (KAUST). W.X. is funded by NSF Materials Research Science and Engineering Center at the university of Minnesota under Grant No. DMR-0819885.

*asalleo@stanford.edu

- ¹M. E. Gershenson, V. Podzorov, and A. F. Morpurgo, *Rev. Mod. Phys.* **78**, 973 (2006).
- ²C. Goldmann, S. Haas, C. Krellner, K. P. Pernstich, D. J. Gundlach, and B. Batlogg, *J. Appl. Phys.* **96**, 2080 (2004).
- ³P. Mark and W. Helfrich, *J. Appl. Phys.* **33**, 205 (1962).
- ⁴V. C. Sundar, J. Zaumseil, V. Podzorov, E. Menard, R. L. Willett, T. Someya, M. E. Gershenson, and J. A. Rogers, *Science* **303**, 1644 (2004).
- ⁵A. L. Briseno, S. C. B. Mannsfeld, M. M. Ling, S. Liu, R. J. Tseng, C. Reese, M. E. Roberts, Y. Yang, F. Wudl, and Z. Bao, *Nature (London)* **444**, 913 (2006).
- ⁶S. Haas, A. F. Stassen, G. Schuck, K. P. Pernstich, D. J. Gundlach, B. Batlogg, U. Berens, and H. J. Kirner, *Phys. Rev. B* **76**, 115203 (2007).
- ⁷S. Nespurek and J. Sworakowski, *J. Appl. Phys.* **51**, 2098 (1980).
- ⁸B. Bohnenbuck, E. von Hauff, J. Parisi, C. Deibel, and V. Dyakonov, *J. Appl. Phys.* **99**, 024506 (2006).
- ⁹S. Berleb, A. G. Mückel, W. Brütting, and M. Schworer, *Synth. Met.* **111–112**, 341 (2000).
- ¹⁰C. Krellner, S. Haas, C. Goldmann, K. P. Pernstich, D. J. Gundlach, and B. Batlogg, *Phys. Rev. B* **75**, 245115 (2007).
- ¹¹J. Dacuña and A. Salleo, *Phys. Rev. B* **84**, 195209 (2011).
- ¹²N. I. Craciun, J. J. Brondijk, and P. W. M. Blom, *Phys. Rev. B* **77**, 035206 (2008).
- ¹³Y. Shen, A. Hosseini, M. Wong, and G. Malliaras, *ChemPhysChem* **5**, 16 (2004).
- ¹⁴R. W. I. de Boer and A. F. Morpurgo, *Phys. Rev. B* **72**, 073207 (2005).
- ¹⁵R. W. I. de Boer, M. Jochemsen, T. M. Klapwijk, A. F. Morpurgo, J. Niemax, A. K. Tripathi, and J. Pflaum, *J. Appl. Phys.* **95**, 1196 (2004).
- ¹⁶R. A. Laudise, C. Kloc, P. G. Simpkins, and T. Siegrist, *J. Cryst. Growth* **187**, 449 (1998).
- ¹⁷O. D. Jurchescu, A. Meetsma, and T. T. M. Palstra, *Acta Crystallogr. B* **62**, 330 (2006).
- ¹⁸B. D. Chapman, A. Checco, R. Pindak, T. Siegrist, and C. Kloc, *J. Cryst. Growth* **290**, 479 (2006).
- ¹⁹J. Hwang, A. Wan, and A. Kahn, *Mater. Sci. Eng., R* **64**, 1 (2009).
- ²⁰A. Salleo, T. W. Chen, A. R. Völkel, Y. Wu, P. Liu, B. S. Ong, and R. A. Street, *Phys. Rev. B* **70**, 115311 (2004).
- ²¹A. R. Völkel, R. A. Street, and D. Knipp, *Phys. Rev. B* **66**, 195336 (2002).
- ²²K. P. Pernstich, B. Rossner, and B. Batlogg, *Nat. Mater.* **7**, 321 (2008).
- ²³D. Oberhoff, K. Pernstich, D. Gundlach, and B. Batlogg, *IEEE Trans. Electron Devices* **54**, 17 (2007).
- ²⁴G. Horowitz, M. E. Hajlaoui, and R. Hajlaoui, *J. Appl. Phys.* **87**, 4456 (2000).
- ²⁵S. Scheinert, K. P. Pernstich, B. Batlogg, and G. Paasch, *J. Appl. Phys.* **102**, 104503 (2007).
- ²⁶A. Troisi, *J. Chem. Phys.* **134**, 034702 (2011).
- ²⁷H. Sirringhaus, *Adv. Mater.* **21**, 3859 (2009).
- ²⁸D. J. Venzon and S. H. T. Moolgavkar, *J. R. Stat. Soc. C (Applied Statistics)* **37**, 87 (1988).
- ²⁹C. Tanase, E. J. Meijer, P. W. M. Blom, and D. M. de Leeuw, *Phys. Rev. Lett.* **91**, 216601 (2003).
- ³⁰S. V. Novikov, D. H. Dunlap, V. M. Kenkre, P. E. Parris, and A. V. Vannikov, *Phys. Rev. Lett.* **81**, 4472 (1998).
- ³¹N. Tessler and Y. Roichman, *Organic Electronics* **6**, 200 (2005).
- ³²O. D. Jurchescu, J. Baas, and T. T. M. Palstra, *Appl. Phys. Lett.* **84**, 3061 (2004).
- ³³O. Mitrofanov, D. V. Lang, C. Kloc, J. M. Wikberg, T. Siegrist, W.-Y. So, M. A. Sergent, and A. P. Ramirez, *Phys. Rev. Lett.* **97** (2006).
- ³⁴H. Najafav, D. Mastrogianni, E. Garfunkel, L. C. Feldman, and V. Podzorov, *Adv. Mater.* **23**, 981 (2011).